Jinwook Kim
Mem. ASME

Changbeom Park

Jongwon Kim
Mem. ASME

F. C. Park[1]
Mem. ASME

School of Mechanical
and Aerospace Engineering,
Seoul National University,
Seoul 151-742, Korea

Performance Analysis of Parallel Mechanism Architectures for CNC Machining Applications

In this paper we propose a set of criteria to evaluate the performance of various parallel mechanism architectures for CNC machining applications. In the robotics literature mathematical formulations of qualities like manipulability, stiffness, and workspace volume have been proposed to evaluate the performance of general-purpose robots. Here we propose a set of performance measures that specifically address features of the machining process. We define precise notions of machine tool workspace, joint and link stiffness, and position and orientation manipulability. The performance of various existing 6 d.o.f. architectures are evaluated with these measures. The analytical methodology presented here, in combination with a graphics-based CAD software environment, can serve as a useful tool in the design of high-performance parallel mechanism machine tools.
[S1087-1357(00)01804-9]

1 Introduction

Parallel mechanisms such as the Stewart-Gough Platform [1] are widely believed to possess a number of advantages over their serial counterparts. Because the moving platform is actuated in parallel by several ''simple'' serial mechanisms, the resulting motion will in general be faster and more accurate than that of serial mechanisms, although at a cost in reduced workspace. It is also commonly believed that parallel mechanisms have superior stiffness characteristics, and are able to carry higher payloads. Seizing upon these perceived advantages over serial structures, several machine tool manufacturers (e.g., Giddings & Lewis, Ingersoll, Toyoda Seiki, Hitachi Seiki) have developed commercial machining centers based on the Stewart-Gough platform architecture, and many more appear likely to follow suit.

Parallel mechanisms have also received a great deal of attention in the robotics literature, particularly with respect to their kinematic analysis and performance evaluation. It is not surprising that most existing numerical criteria used for evaluating a parallel mechanism's kinematic performance are directly adopted from robotics contexts. In particular, two performance criteria that have been the object of a great deal of research are a mechanism's *workspace* and *manipulability*. Several mathematical formulations of these criteria have been proposed, most of which are variations on a common theme (see, e.g., [2,3]). Existing studies usually address open chains, however, and the few that treat closed chains limit their attention to modifications of the standard Stewart-Gough Platform design (e.g., varying the platform dimensions, or relocating the positions at which the legs are attached to the platforms [4,5]).

While the above performance criteria are in most cases sufficient for robots, machine tools demand a more specific set of criteria. In particular, the stiffness requirements for machine tools cannot be overemphasized. In this article we modify the set of existing robot performance criteria to reflect the particular needs of machine tools, and evaluate the suitability of various architectures as mechanical platforms for universal machining centers. Specifically, we develop the notion of machine tool workspace, which captures the maximal size of the workpiece that can be machined while considering joint limits and link interference (which can be critical for parallel mechanisms). Our definition also accounts for the fact that, for machine tools, rotation about the spindle axis can be regarded as a redundant degree of freedom. We also analyze joint stiffness by taking advantage of its duality with the traditional robotic concept of manipulability, and develop a simple method for analyzing the first-order structural stiffness characteristics of parallel mechanisms without resorting to computationally expensive and time-consuming FEM analysis. Somewhat surprisingly, a unified analysis of joint and link stiffness of parallel mechanisms is a subject that has received only scant attention in the literature (e.g., [1]), despite its obvious importance to machining applications.

The paper is organized as follows. In Section 2 we define and explain the mathematical formulations for manipulability, joint and link stiffness, and machine tool workspace. In Section 3 we compare, using the criteria developed in this paper, the performance of two six degree-of-freedom parallel mechanisms: the conventional Stewart-Gough Platform, and the PRPS $\times 3$ Mechanism, a hybrid six degree of freedom serial-parallel structure. The proposed criteria offer a means of directly comparing the performance of various parallel mechanism architectures, as well as of numerically optimizing existing designs. Given the large variety of possible architectures for parallel mechanisms, it is our belief that a better understanding and quantification of machine performance is crucial to developing future machine tools based on the parallel mechanism architecture.

2 Performance Measures for Parallel Mechanisms

2.1 Manipulability. The qualitative idea behind the concept of manipulability is the ability of a mechanism to move and apply forces in arbitrary directions as easily as possible. The use of manipulability as a robotic performance measure can be traced back to Salisbury and Craig [6], who determined the optimal link lengths for a three-link planar finger with respect to this measure. The major axis of the manipulability ellipsoid indicates the direction along which the mechanism can move with the least effort, while the minor axis indicates the direction along which the mechanism is stiffest, i.e., the mechanism's actuators can resist forces with minimum effort along these directions.

The manipulability ellipsoid formulation proceeds as follows. Let θ be the vector of active joints, and $J(\theta)$ be the Jacobian that relates actuated joint velocities to the tip's angular velocity ω and linear velocity v:

$$\begin{bmatrix} \omega \\ v \end{bmatrix} = \begin{bmatrix} J_\omega(\theta) \\ J_v(\theta) \end{bmatrix} \dot{\theta} = J(\theta)\dot{\theta} \tag{1}$$

[1]Corresponding author, E-mail: fcp@plaza.snu.ac.kr

Contributed by the Manufacturing Engineering Division for publication in the JOURNAL OF MANUFACTURING SCIENCE AND ENGINEERING. Manuscript received Jan. 1997; revised Dec. 1999. Associate Technical Editor: K. Ehmann.

The manipulability ellipsoid is determined from the eigenvalues and eigenvectors of JGJ^T, where G is a diagonal weighting matrix whose elements reflect the physical characteristics of the actuators (see [7]). For example, from virtual work considerations the square root of the ith diagonal element of G, $\sqrt{g_i}$, can be regarded as representing the peak velocity of the ith actuator.

One common and fatal mistake made in past approaches is to combine position and orientation information into a single scalar manipulability measure. For example, the condition number $\lambda_{max}/\lambda_{min}$, where λ_{max} and λ_{min} respectively are the largest and smallest eigenvalues of JGJ^T, has been a popular choice for a manipulability objective function (when $\lambda_{max}/\lambda_{min}$ attains the minimum possible value of 1, the manipulability ellipsoid becomes spherical). It is physically inconsistent, however, to combine orientation and position information in such a fashion; all such measures ultimately involve some sort of tradeoff between orientation and position, and it is well-known that no natural length scale for physical space exists (see, e.g., [8,9] for a rigorous mathematical discussion).

For our purposes, we choose to analyze orientation and position manipulability separately rather than weighting them in some ad-hoc fashion. That is, we construct separate manipulability ellipsoids for $J_v(\theta)$ and $J_\omega(\theta)$, and use this information as a design guide. In this case the principal axes of $J_\omega(\theta)$ correspond to axes about which rotation is either the easiest (major axes) or most difficult (minor axes). For analyzing the manipulability of parallel mechanisms whose actuators exceed the kinematic degrees of freedom, see [10].

2.2 Joint and Link Stiffness. The structural stiffness of a mechanism is affected both by joint and link deflections. Depending on the mechanism, the contribution of these deflections may vary considerably. For most industrial robots with their rugged designs, joint deflections tend to dominate, whereas link deflections are more dominant for mechanisms employing lightweight composite-type materials. For accurate stiffness analysis of parallel mechanisms it is necessary to consider both types of deflections.

There have been several theoretical studies on the compliance of rigid bodies joined by elastic couplings (e.g., linear springs) [11–13]. Most of these approaches begin by assuming a potential function for the system that is a function of position only, and define the stiffness matrix to be the Hessian of the potential function. While the focus of these papers is primarily on the mathematical characteristics of the stiffness and compliance matrices, our focus is rather on the determination of this potential function for general parallel mechanisms, taking into account joint deflections and strain energy of each of the deformed links.

Assuming linear models of joint deflection, joint stiffness can be modeled quite easily within the earlier manipulability framework. Specifically, from the same virtual work considerations the ith diagonal entry of G, $\sqrt{g_i}$, can be regarded as the spring constant associated with the ith actuated joint (see, e.g., [7]). With this interpretation of G the resulting ellipsoid can now be regarded as a stiffness ellipsoid: the minor axis indicates directions along which the manipulator is the stiffest (or, able to resist forces along this direction with the least effort), which is perpendicular to the most manipulable direction (the major axis). In the event that the actuators are identical, the joint spring constant only acts as a scaling factor to JJ^T, and produces the exact same results as the manipulability analysis with G set to I.

Link stiffness for parallel mechanisms is more difficult to model, and with only a few exceptions (e.g., [14]) has received very little attention in the literature. Our analysis of structural stiffness will focus on the *compliance* of the parallel mechanism. If a force f and moment m are applied to the tip, then due to the elastic properties of the links the tip will experience a position displacement $dx \in \Re^3$ and orientation displacement $d\Omega \in \Re^3$. Here $d\Omega$ is expressed relative to the tip frame, and determined from the elements of the following skew-symmetric matrix:

$$[d\Omega] = \begin{bmatrix} 0 & -d\Omega_3 & d\Omega_2 \\ d\Omega_3 & 0 & -d\Omega_1 \\ -d\Omega_2 & d\Omega_1 & 0 \end{bmatrix} = R^{-1}\, dR \tag{2}$$

where R is the 3×3 rotation matrix representing the orientation of the tip frame. The first-order linear force-displacement relationship is then given by

$$\begin{bmatrix} d\Omega \\ dx \end{bmatrix} = C \begin{bmatrix} m \\ f \end{bmatrix} \tag{3}$$

where $C \in \Re^6$ is the symmetric *compliance matrix*; note that C depends on the configuration of the mechanism, and is a function of the joint values. For notational convenience we denote the generalized force (m,f) and generalized displacement $(dx,d\Omega)$ by $\mathcal{F}$ and $\delta\mathcal{X}$, respectively: then $d\mathcal{X}=C\mathcal{F}$.

By Castigliano's Theorem one can write

$$d\mathcal{X} = \frac{\partial U}{\partial \mathcal{F}} \tag{4}$$

where U is the total strain energy of the mechanism. The total strain energy in turn can be found from the following formula. First, for each link i let A_i denote the cross-sectional area, E_i be Young's modulus, G_i the shear modulus, $I_{z,i}$ the axial moment of inertia, I_i the radial moment of inertia, and L_i the link length. Further, let f_i be the component of the link internal force along the axial direction, $m_{b,i}$ the bending moment, and $m_{t,i}$ the torsional moment. Then assuming a total of n links,

$$U = \sum_{i=1}^{n} \int_{L_i} \frac{m_i^2}{2A_iE_i}\,dx + \int_{L_i} \frac{m_{b,i}^2}{2E_iI_i}\,dx + \int_{L_i} \frac{m_{t,i}^2}{2G_iI_{z,i}}\,dx \tag{5}$$

Also realizing that U can be written as $U=\frac{1}{2}\mathcal{F}^TC\mathcal{F}$, the system compliance matrix C can be found by differentiating U with respect to generalized force. Observe that the stiffness matrix K is then defined to be C^{-1} (when it exists).

The ellipsoid associated with the stiffness matrix K can be interpreted in a similar fashion to the manipulability ellipsoid. The major and minor axes are given by the eigenvalues and eigenvectors of K, and indicate directions along which the mechanism as a structure is the most and least stiff. As with manipulability, it is inconsistent to combine quantities with different physical units, and hence we analyze the individual components of the compliance ellipsoid separately, i.e., for

$$\begin{bmatrix} d\Omega \\ dx \end{bmatrix} = \begin{bmatrix} C_{11} & C_{12} \\ C_{21} & C_{22} \end{bmatrix} \begin{bmatrix} m \\ f \end{bmatrix} \tag{6}$$

we examine the ellipsoids for each C_{ij} separately.

2.3 Machine Tool Workspace. The workspace of a mechanism refers to the set of all positions and orientations achievable by the tip frame. In the robotics literature the workspace is often classified into two components, the *reachable* and *dexterous* workspace. The reachable workspace is defined to be the set of points in physical space that can be reached by the tip (or more precisely, the origin of the tip frame). The dexterous workspace on the other hand is the set of points that can be reached with any arbitrary orientation of the tip frame.

One disadvantage of this classification is that there is no means of smoothly trading off orientation freedom for position freedom. Differential geometric methods can overcome this disadvantage, by introducing a volume form on the space of homogeneous transformations. This volume form can be visualized as follows. Suppose a machine tool is restricted to move within a cube of space of length 1 m on each side. At each point within this cube the spindle can point itself anywhere in a 4π solid angle and rotate 2π about the direction it is pointing. The orientation volume at such a point

is $4\pi \times 2\pi = 8\pi^2$ radian^3. Multiplying by the positional volume one obtains $8\pi^2$ radian^3 m^3 for the volume of the free configuration space of the machine tool. This is the geometric notion of workspace volume on the homogeneous transformations: we refer the reader to [7] for the mathematical details and computational formulas.

While this notion of workspace volume has the advantage of being fixed and moving frame invariant, as well as being mathematically precise, parallel mechanisms that maximize this volume measure may not necessarily be well-suited for machining applications. Since one of our goals is to be able to machine a given workpiece over as large an area of its surface as possible, it is not necessary that the spindle be able to assume arbitrary orientations over the widest range of the Cartesian workspace. Rather, one should take into account the fact that the workpiece will typically be placed at the center of the workspace, and that spindle access to the lower surface in contact with the worktable is not necessary.

Suppose a reference frame is attached to the spindle in such a fashion that the z-axis is directed along the spindle axis. Define the rotation angles about the x, y, and z axes by α, β, and γ. Borrowing machine tool terminology, we shall also refer to α, β, and γ as the spindle *turning*, *tilting*, and *rotation* angles, respectively. Note that the rotation angle γ is irrelevant for machining purposes, and can be regarded as a redundant degree of freedom. The z-axis of the fixed frame is assumed to be directed vertically upward. Suppose that the workpiece to be machined is a cube. A more practical workspace requirement for machining applications, then, is that the spindle be able to access all points on the top and 4 side faces of the cylinder while the spindle is orthogonal to the surface. Moreover, while the spindle tip maintains contact with an arbitrary point of the workpiece, we would like the spindle to be able to rotate 360 degrees about the fixed frame z-axis.

Most existing parallel mechanism designs will of course not be able to achieve the above workspace capability, due to mechanical constraints such as joint limits and link interference, as well as the presence of kinematic singularities. What we would like is a notion of workspace that attempts to capture how close a mechanism comes to achieving this capability. With such an objective in mind, we define the following notion of a machine tool's workspace. First, the *positioning workspace for spindle tilting angle* β refers to the set of all points in Cartesian space with respect to which the spindle can rotate 360 deg about the fixed frame z-axis (with the spindle tip maintaining contact with the point in question), while the spindle is tilted at an angle of β with respect to the vertical ($\beta = 0$ deg indicates a vertical spindle, suitable for machining the top surface of the cube, while β should be set to 90 deg in order to machine the side faces). Figure 1 graphically illustrates this concept of positioning workspace. As mentioned earlier, because of mechanical constraints most existing parallel mechanism designs have a limited spindle tilting angle, typically a maximum β of approximately 30 deg.

To calculate the machine tool workspace as described above for actual mechanisms, it is extremely important (especially for parallel mechanisms) to keep in mind the physical constraints at work: joint limits for prismatic, revolute, and spherical joints, as well as interference between the links. Of the three types of joints considered, our experience indicates that in general spherical joint limits tend to be the most dominant in determining a mechanism's workspace.

3 Six D.O.F. Parallel Mechanism Performance

In this section we examine the manipulability, link stiffness, and machine tool workspace characteristics of two 6 dof freedom parallel mechanism designs: the conventional Stewart-Gough Platform, and the 3-PRPS Mechanism, a hybrid serial-parallel structure first proposed by Behi [15] and also developed independently by the authors.

3.1 Stewart-Gough Platform. The particular Stewart-Gough Platform whose performance we evaluate is illustrated in Figure 2. The stationary and mobile platforms are connected by 6 elementary chains of type S-P-S, with the P joint actuated. As previously indicated, several machine tools based on this architecture have already been commercialized by, e.g., Ingersoll, Giddings, and Lewis [16]. The platform we consider has the following dimensions (all units of length are in millimeters): stationary platform radius=235, mobile platform radius=135, actuator stroke range=[300,500], height of mobile platform in home posture=400, ball joint range=55 deg. For the given kinematic parameters the maximum tilting angle (which in this case is determined by the ball joint range) is determined to be 46 deg. The fixed frame is located at the center of the stationary platform, with its z-axis normal to the platform and pointing up. For convenience the spindle tip is assumed to coincide with the origin of the moving platform.

Figures 2 and 3 show the position and orientation manipulability ellipsoids in the home posture, respectively, while Figures 4 and 5 show the respective position and orientation link stiffness ellipsoids at the home posture. As expected, the Stewart-Gough Platform shows high stiffness along the vertical direction, which implies good manipulability characteristics in the horizontal plane. It is also slightly stiffer to rotations about axes lying in the $x-y$ plane than the z-axis, which indicates better manipulability for rotations about the vertical z-axis.

Figures 6–9 depict side and top views of the position workspace for various tilting angles ranging from 0 deg to 40 deg; recall that for the chosen platform kinematic parameters, the

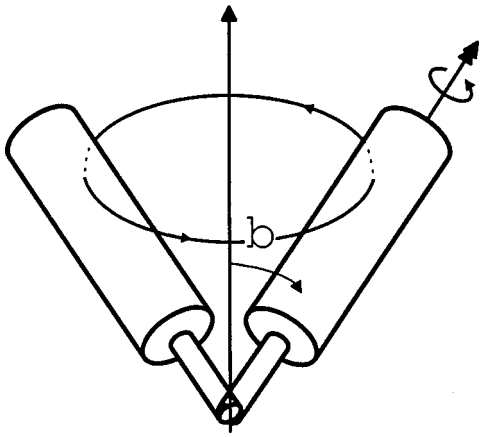

Fig. 1 The concept of machine tool workspace for tilting angle β

Fig. 2 Position manipulability ellipsoid of Stewart-Gough Platform in the home posture

Fig. 3 Orientation manipulability ellipsoid of Stewart-Gough Platform in the home posture

Fig. 4 Position stiffness ellipsoid of Stewart-Gough Platform in the home posture

Fig. 5 Orientation stiffness ellipsoid of Stewart-Gough Platform in the home posture

maximum tilting angle is 46 deg. It is interesting to observe the sharp decrease in the workspace volume with increasing tilting angle; for machining tasks that require spindle tilting angles in excess of 20 deg one is usually limited to a workspace approximately the size of the mobile platform. Note also the unusual shape evolution of the workspace cross-section as the mobile platform approaches the stationary platform.

3.2 3-PRPS Mechanism. The six degree of freedom 3-PRPS Mechanism (Figure 10) is composed of 3 elementary chains, each of type PRPS. Only the P joints are actuated. Each of the 3 vertical legs slides along the horizontal rails attached to the

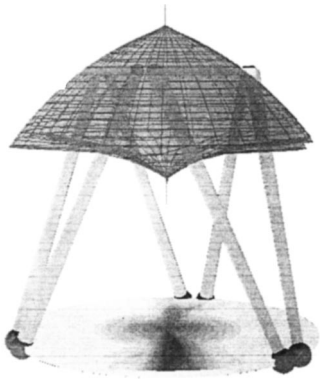

Fig. 6 Position workspace of Stewart-Gough Platform for tilting angle 0 deg, side view

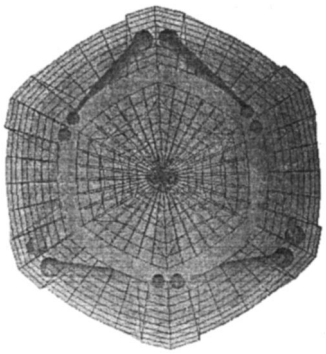

Fig. 7 Position workspace of Stewart-Gough Platform for tilting angle 0 deg, top view

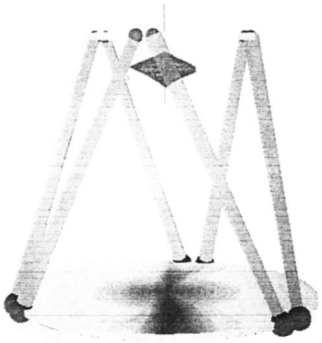

Fig. 8 Position workspace of Stewart-Gough Platform for tilting angle 40 deg, side view

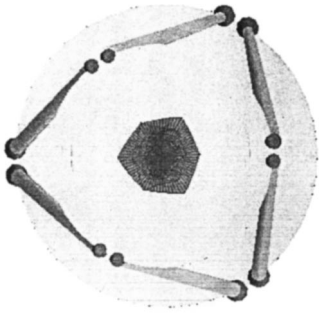

Fig. 9 Position workspace of Stewart-Gough Platform for tilting angle 40 deg, top view

base; the 3 vertical legs in turn have variable lengths. The dimensions of the mechanism are as follows: the radius of the stationary lower platform is 235, the upper mobile platform has radius 50, the joint range of the vertical legs is 200–400, and the ball joints have a maximum range of 55 deg. As with the Stewart-Gough

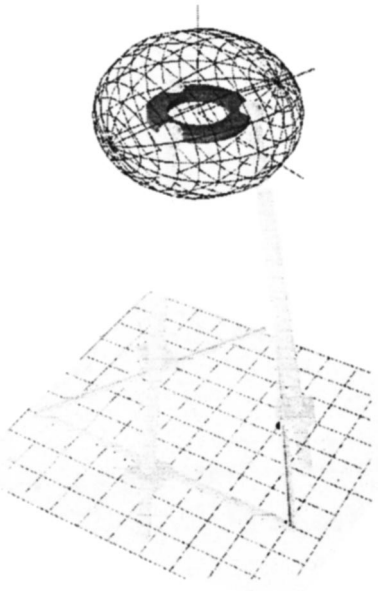

Fig. 10 Position manipulability ellipsoid of the 3-PRPS Mechanism in the home posture

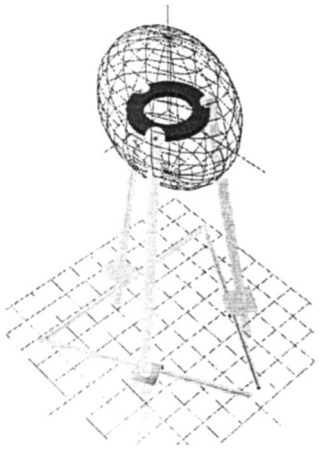

Fig. 11 Orientation manipulability ellipsoid of the 3-PRPS Mechanism in the home posture

Platform, at the home posture the upper platform is at a height of 400. Also, for convenience the spindle tip is assumed to coincide with the center of the mobile platform.

Figures 10 and 11 show the position and orientation manipulability ellipsoids of the 3-PRPS Mechanism in the home posture, respectively, while Figures 12 and 13 show the respective position and orientation link stiffness ellipsoids at the home posture. Both the position and orientation manipulability ellipsoids are quite uniform with respect to all directions. The orientation stiffness ellipsoid is also reasonably uniform, but the position stiffness ellipsoid indicates that stiffness along directions in the x-y plane is relatively low compared to that along the z-axis. This result would seem to agree with our intuition about the structural properties of the 3-PRPS Mechanism, especially when contrasted with the results obtained previously for the Stewart-Gough Platform.

Figures 14–17 depict side and top views of the position workspace for various tilting angles ranging from 0 deg to 45 deg; that for the chosen kinematic parameters, the maximum tilting angle of the 3-PRPS Mechanism is 52 deg, or about 6 degrees greater than that of the Stewart-Gough Platform. In general the positioning workspace volume of the 3-PRPS Mechanism is much larger than that of the Stewart-Gough Platform assuming machines of approximately the same physical dimension. It is also interesting here to observe the sharp decrease in the workspace volume with

Fig. 12 Position stiffness ellipsoid of the 3-PRPS mechanism in the home posture

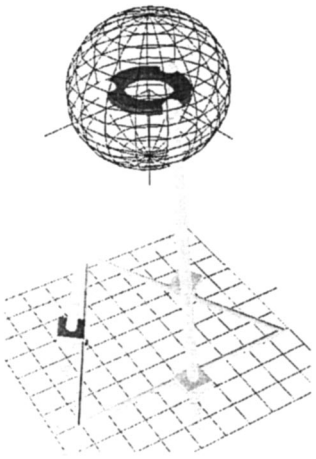

Fig. 13 Orientation stiffness ellipsoid of the 3-PRPS Mechanism in the home posture

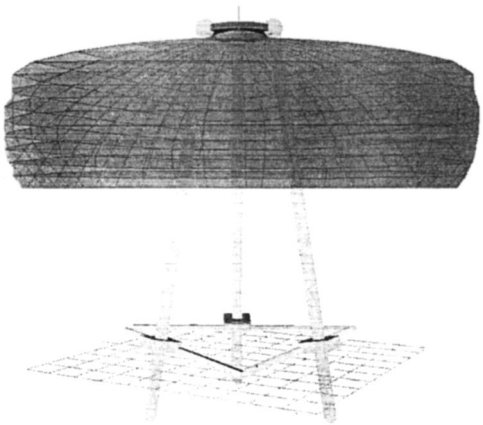

Fig. 14 Position workspace of the 3-PRPS Mechanism for tilting angle 0 deg, side view

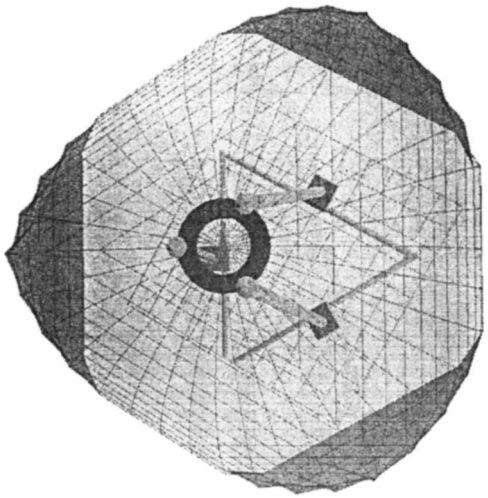

Fig. 15 Position workspace of the 3-PRPS Mechanism for tilting angle 0 deg, top view

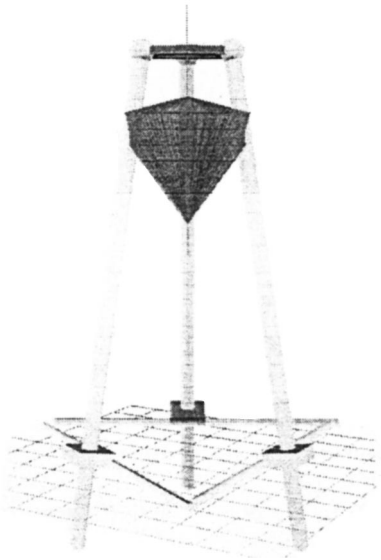

Fig. 16 Position workspace of the 3-PRPS Mechanism for tilting angle 40 deg, side view

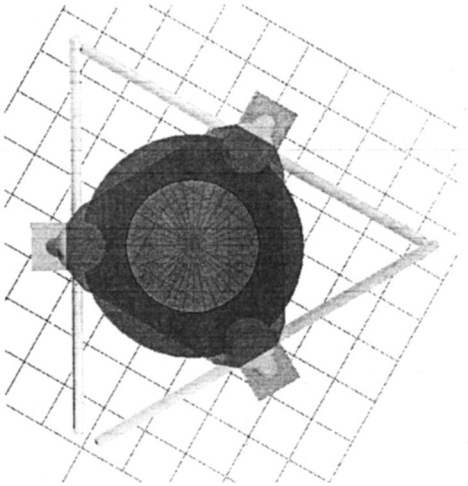

Fig. 17 Position workspace of the 3-PRPS Mechanism for tilting angle 40 deg, top view

increasing tilting angle. In contrast to the Stewart-Gough Platform, one does not find the unusual shape evolution of the workspace cross-section as the mobile platform approaches the stationary platform; the triangular shape of the cross-section is maintained throughout.

4 Conclusions

In this paper we have presented a set of criteria to evaluate the performance of various parallel mechanism architectures for CNC machining applications. Borrowing notions from robotics as our point of departure, we have identified a more specific set of performance measures that takes into account the unique features of the machining process. Precise notions of machine tool workspace, joint and link stiffness, and position and orientation manipulability have been defined, and the performance of two 6 d.o.f. designs, the Stewart-Gough Platform and the 3-PRPS Mechanism, were evaluated with respect to these measures.

In comparing mechanisms of different topologies, it is important to keep in mind which measures are invariant with respect to

topology. For example, given the physical dimensions of two mechanisms, a direct and meaningful comparison of machine tool workspace can be made between the two mechanisms regardless of their topologies. For a comparison of the stiffness and manipulability ellipsoids for mechanisms of different topologies, one must be careful when drawing conclusions based on the actual ellipsoid sizes; in particular, the physical units of all numerical quantities must be considered carefully when the actuated joints of the two mechanisms are of different types. The shape of the ellipsoids are always meaningful, however, and provide valuable information regarding the directions of maximum and minimum stiffness, accuracy, etc.

Although the parallel mechanisms considered in this paper all have the same number of actuated joints as degrees of freedom, future parallel mechanisms may be antagonistically actuated and redundant—overactuation and kinematic redundancy offer a means of overcoming the problems of limited workspace and singularities associated with parallel mechanisms. For such mechanisms the manipulability and stiffness analyses above requires some modification: differential geometric methods in particular are an effective means for addressing overactuated mechanisms [10,17].

Acknowledgements

This research was supported in part by the National Research Lab for CAD/CAM, and by the National Research Group for Order-Adaptive Rapid Product Development.

References

[1] Stewart, D., 1966, ''A platform with six degrees of freedom,'' Proc. Inst. Mech. Eng., **180**, Part I, No. 15, pp. 371–386.

[2] Yoshikawa, T., 1985, ''Manipulability of robotic mechanisms,'' Int. J. Robot. Res., **4**, No. 2, pp. 3–9.

[3] Klein, C. A., and Blaho, B., 1987, ''Dexterity measures for the design and control of kinematically redundant manipulators,'' Int. J. Robot. Res., **6**, No. 2, pp. 72–83.

[4] Stoughton, R., and Arai, T., 1993, ''A modified Stewart platform manipulator with improved dexterity,'' IEEE Trans. Rob. Autom., **9**, No. 2, pp. 166–173.

[5] Gosselin, C. M., and Angeles, J., 1988, ''The optimum kinematic design of a planar three-degree-of-freedom parallel manipulator,'' ASME J. Mech., Transm., Autom. Des., **110**, pp. 35–41.

[6] Salisbury, J. K., and Craig, J. J., 1982, ''Articulated hands: force control and kinematic issues,'' Int. J. Robot. Res., **1**, No. 1, pp. 4–17.

[7] Park, F. C., 1995, ''Optimal robot design and differential geometry,'' Trans. ASME 50th Anniv. Special Issue, **117**(B), pp. 87–92.

[8] Duffy, J., 1990, ''The fallacy of modern hybrid control theory that is based on 'orthogonal complements' of twist and wrench spaces,'' J. Rob. Syst., **7**, No. 2, pp. 139–144.

[9] Park, F. C., 1995, ''Distance metrics on the rigid-body motions with applications to mechanism design,'' ASME J. Mech. Des., **117**, No. 1, pp. 48–54.

[10] Park, F. C., and Kim, J. W., 1998, ''Manipulability of closed kinematic chains,'' ASME J. Mech. Des., **120**, No. 4, pp. 542–548.

[11] Griffis, M., and Duffy, J., 1993, ''Global stiffness modeling of a class of simple compliant couplings,'' Mech. Mach. Theory, **28**, No. 2.

[12] Patterson, T., and Lipkin, H., 1993, ''Structure of robot compliance,'' ASME J. Mech. Des., **115**, No. 3, pp. 576–580.

[13] Loncaric, J., 1987, ''Normal forms of stiffness and compliance matrices,'' IEEE Trans. Rob. Autom., **3**, No. 6, pp. 567–572.

[14] Bhattarchaya, S., Hatwal, H., and Ghosh, A., 1995, ''On the optimum design of Stewart platform type parallel manipulators,'' Robotica, **13**, pp. 133–140.

[15] Behi, F., 1988, ''Kinematic analysis for a six degree-of-freedom 3-PRPS parallel mechanism,'' IEEE J. Rob. Autom., **4**, No. 5, pp. 561–565.

[16] Valenti, M., 1995, ''Machine tools get smarter,'' ASME Mech. Eng., **117**, No. 11, pp. 70–75, November.

[17] Park, F. C., and Kim, J. W., 1999, ''Singularity analysis of closed kinematic chains,'' ASME J. Mech. Des., **121**, No. 1 (to appear).